

Dear authors,

Thank you very much for your contribution to Chinese Physics B.

Your paper has been published in Chinese Physics B, 2014, Vol.23, No.5.

Attached is the PDF offprint of your published article, which will be convenient and helpful for your communication with peers and coworkers.


Readers can download your published article through our website

<http://www.iop.org/cpb> or <http://cpb.iphy.ac.cn>

What follows is a list of related articles published recently in Chinese Physics B.


[Ho and Ti co-doped BiFeO₃ multiferroic ceramics with enhanced magnetization and ultrahigh electrical resistivity](#)

Gu Yan-Hong, Liu Yong, Yao Chao, Ma Yan-Wei, Wang Yu, Chan Helen Lai-Wah, Chen Wan-Ping

Chin. Phys. B . 2014, 23(3): 037501. Full Text:  [PDF](#) (906KB)


[A quantum explanation of the magnetic properties of Mn-doped graphene](#)

Lei Tian-Min, Liu Jia-Jia, Zhang Yu-Ming, Guo Hui, Zhang Zhi-Yong

Chin. Phys. B . 2013, 22(11): 117502. Full Text:  [PDF](#) (899KB)


[Effect of vanadium on the room temperature ferromagnetism of V-doped 6H-SiC powder](#)

Wang Hui, Yan Cheng-Feng, Kong Hai-Kuan, Chen Jian-Jun, Xin Jun, Shi Er-Wei

Chin. Phys. B . 2013, 22(2): 027505. Full Text:  [PDF](#) (298KB)


[Multiferroic phase transitions in manganites RMnO₃: A two-orbital double exchange simulation](#)

Tao Yong-Mei, Lin Lin, Dong Shuai, Liu Jun-Ming

Chin. Phys. B . 2012, 21(10): 107502. Full Text:  [PDF](#) (221KB)


[Defects mediated ferromagnetism in a V-doped 6H-SiC single crystal](#)

Zhuo Shi-Yi, Liu Xue-Chao, Xiong Ze, Yan Wen-Sheng, Xin Jun, Yang Jian-Hua, Shi Er-Wei

Chin. Phys. B . 2012, 21(6): 067503. Full Text:  [PDF](#) (146KB)

[A first-principles study of the magnetic properties in boron-doped ZnO](#)

Xu Xiao-Guang, Yang Hai-Ling, Wu Yong, Zhang De-Lin, Jiang Yong

Chin. Phys. B . 2012, 21(4): 047504. Full Text:  [PDF](#) (163KB)

中国物理 **B**
**Chinese
Physics B**

Volume 23 Number 5 May 2014

Formerly *Chinese Physics*

A Series Journal of the Chinese Physical Society
Distributed by IOP Publishing

Online: iopscience.iop.org/cpb
cpb.iphy.ac.cn

CHINESE PHYSICAL SOCIETY
IOP Publishing |

Effect of Gd doping on the magnetism and work function of $\text{Fe}_{1-x}\text{Gd}_x/\text{Fe}$ (001)*

Tang Ke-Qin(汤可鞞), Zhong Ke-Hua(钟克华), Cheng Yan-Ming(程燕铭), and Huang Zhi-Gao(黄志高)[†]

College of Physics and Energy, Fujian Normal University, Fujian Provincial Key Laboratory of Quantum Manipulation and New Energy Materials, Fuzhou 350108, China

(Received 3 August 2013; revised manuscript received 23 October 2013; published online 25 March 2014)

The magnetism and work function Φ of $\text{Fe}_{1-x}\text{Gd}_x/\text{Fe}$ (001) films have been investigated using first-principles methods based on the density functional theory. The calculated results reveal that Gd doping on the Fe (001) surface would greatly affect the geometrical structure of the system. The reconstruction of the surface atoms leads to the transition of magnetic coupling between Gd and Fe atoms from ferromagnetic (FM) for $0.5 \leq x \leq 0.75$ to antiferromagnetic (AFM) for $x = 1.0$. For $\text{Fe}_{1-x}\text{Gd}_x/\text{Fe}$ (001) ($x = 0.25, 0.5, 0.75, 1.0$), the charge transfer from Gd to Fe leads to a positive dipole formed on the surface, which is responsible for the decrease of the work function. Moreover, it is found that the magnetic moments of Fe and Gd on the surface layer can be strongly influenced by Gd doping. The changes of the work function and magnetism for $\text{Fe}_{1-x}\text{Gd}_x/\text{Fe}$ (001) can be explained by the electron transfer, the magnetic coupling interaction between Gd and Fe atoms, and the complex surface reconstruction. Our work strongly suggests that the doping of the metal with a low work function is a promising way for modulating the work function of the magnetic metal gate.

Keywords: first-principles method, doping, magnetism, work function

PACS: 63.20.dk, 75.70.-i, 65.40.gh, 75.50.Bb

DOI: 10.1088/1674-1056/23/5/056301

1. Introduction

Magnetic tunnel junctions have become important components appearing in magnetic random-access memory, the read heads of magnetic disks, and semiconductor-based spin devices. Inserting a tunnel barrier has become a key method to achieve the spin injection. However, spin injection into Si is still elusive because the Schottky barrier formation leads to a huge conductivity mismatch of the ferromagnetic (FM) tunnel contact and Si,^[1] which is detrimental to spin transport and spin injection. Moreover, it cannot be solved by adjusting the tunnel barrier thickness.^[2,3] An accepted route to overcome the electrical mismatch and prevent interfacial chemical reactions is to employ the tunneling of spins through an oxide barrier such as Al_2O_3 .^[4] Min *et al.* presented a radically different approach for spin-tunneling resistance control using low-work-function ferromagnet Gd ($\Phi = 3.1$ eV) inserted at the FM/tunnel barrier interface.^[5] It was found that in this way, the resistance–area (RA) product of FM/ Al_2O_3 /Si contacts can be tuned over eight orders of magnitude, while simultaneously maintaining a reasonable tunnel spin polarization. It was also suggested that the lowering effective work function of the FM by inserting Gd is related to the structure and the magnetism at the Fe/Gd interface. Recently, the effect of a ferromagnetic Gd marker layer on the effective work function of Fe in a Fe/Gd/ Al_2O_3 /Si stack has been systematically investigated.^[6] When the Gd marker thickness was changed from 0 nm to 2.7 nm, the measured effective work function of

Fe at the Fe/Gd/ Al_2O_3 interface was reduced from 4.5 eV to 3.7 eV. Moreover, from ⁵⁷Fe conversion electron Mossbauer spectroscopy, a certain degree of Fe–Gd mixing at the interface was observed. It was also suggested that, with increasing Gd interlayer thicknesses, the lowering effective work function of Fe is related to the changes of the structure and magnetism in the Fe/Gd interface. The work function can be tuned by several methods. For example, the alloying modulation of the work functions for binary alloys has been studied in experiments and theories.^[7–11] Xu *et al.* have revealed that the surface alloy composition and the surface orientation can affect the work functions of MoTa and NiPt systems in a distinctive fashion.^[10,11] Also, Park *et al.* have found that the submonolayer of an overlying metal can significantly affect the work functions of NiAl and PtAl systems.^[12] However, up to now, the impact of Gd doping on the work function of the $\text{Fe}_{1-x}\text{Gd}_x/\text{Fe}$ surface has not been studied well. In this paper, based on first principles calculation, we investigate the effect of Gd doping on the magnetism and work function of $\text{Fe}_{1-x}\text{Gd}_x/\text{Fe}$ (001). The calculated results reveal that the geometrical structure of Fe(001) can be greatly affected by Gd doping. The surface reconstruction of atoms leads to the transition of magnetic coupling between Gd atoms from ferromagnetic for $0.5 \leq x \leq 0.75$ to antiferromagnetic (AFM) for $x = 1.0$. Moreover, the work function of $\text{Fe}_{1-x}\text{Gd}_x/\text{Fe}$ (001) can be reduced by Gd doping, and the modulated range reaches 1.12 eV (from 3.86 eV to 2.74 eV).

*Project supported by the National Natural Science Foundation of China (Grant No. 11004039) and the National Basic Research Program of China (Grant No. 2011CBA00200).

[†]Corresponding author. E-mail: zghuang@fjnu.edu.cn

2. Method

The work functions of the $\text{Fe}_{1-x}\text{Gd}_x/\text{Fe}$ (001) surfaces were calculated using a first principles method based on the density-functional theory (DFT).^[13] All calculations were carried out using the Vienna *ab initio* simulation package, employing the generalized gradient approximation (GGA) of Perdew–Burke–Ernzerhof for the exchange–correlation function.^[10,14–22] As Gd is a typical heavy metal, the spin-orbit coupling should be considered. The moderate correlation of 3d electrons and the strong correlation of f electrons in Gd require adding an on-site Coulomb interaction U . In the GGA+ U method,^[23] the parameters U and J represent the on-site Coulomb interaction energy (Hubbard U) and the atomic-orbital intra-exchange energy (Hund’s coupling parameter), respectively. In the calculation, the optimal values of U_{eff} were determined by comparing the calculated magnetic moments with the experimental and other calculated values.^[24–26] Finally, the values of U_{eff} for Fe and Gd were chosen as 0.2 eV and 6.9 eV, respectively. All $\text{Fe}_{1-x}\text{Gd}_x/\text{Fe}$ (001) surfaces were modeled by a nine-layer Gd/Fe slab with a (2×2) unit cell. The supercell contained 36 atoms, where there were 4 atoms in each layer, and the periodic boundary conditions were applied with 15 Å of a vacuum between the slabs. Brillouin-zone integrations had been performed via the Methfessel–Paxton technique^[27] on a $5 \times 5 \times 1$ k mesh. A cutoff energy of 300 eV was used for the plane-wave expansion of the electron

wave function. These parameters ensured a convergence better than 1 meV for the total energy. The atomic coordinates in the supercell were fully relaxed using the conjugate-gradient algorithm^[28] until the maximum Hellmann Feynman force on a single atom was less than 0.02 eV/Å. After relaxation, the work functions were calculated as the differences between the electrostatic potential in the middle of the vacuum region and the metal Fermi energy.^[29]

Our convergence test indicated that a slab consisting of a minimum of four metal layers is required. Subsequent calculations of the work functions of the $\text{Fe}_{1-x}\text{Gd}_x/\text{Fe}$ (001) surfaces were performed using slabs of nine layers and a 2×2 surface unit cell with the four bottom layers being frozen. In order to verify our computational approach, we calculated the lattice constants and magnetic moments M of bulk Fe and Gd, the magnetic moments of the topmost layer atoms M_{sur} , and the work functions Φ for Fe(001) and Gd(001). The calculated results and the corresponding experimental data are listed in Table 1. From the Table, it is found clearly that the calculated lattice constants, magnetic moments, and work functions are consistent with those in experiments and other calculated data from Refs. [30]–[39]. Moreover, our calculated work function of 3.86 eV is slightly less than the experimental value of 4.24 eV, which should be attributed to the strained effect in real films.^[35]

Table 1. Lattice constants and magnetic moments M for bulk Fe and Gd (in GGA and GGA+ U); magnetic moments of the topmost layer atoms M_{sur} and the work functions Φ for Fe (001) and Gd(001).

	Lattice constant/Å			M/μ_B			M_{sur}/μ_B		Φ/eV		
	this work	other calculation	Expt.	this work		Expt.	this work	other calculation	this work	other calculation	Expt.
				GGA	GGA+ U						
Fe	2.830	2.830 ^{a)}	2.703 ^{b)}	2.07	2.20	2.20 ^{c)}	2.98	2.98 ^{d)}	3.86	3.86 ^{e)}	4.24 ^{f)}
Gd	$a = 3.636, c = 5.783$		$a = 3.622, c = 5.74$ ^{g)}	7.50	7.63	7.63 ^{h)}	7.73	7.77 ⁱ⁾	2.9		3.1 ^{j)}

^{a)}Ref. [30]; ^{b)}Ref. [31], experimental lattice constant is extrapolated to $T = 0$ K; ^{c)}Ref. [32]; ^{d)}Ref. [33]; ^{e)}Ref. [34]; ^{f)}Ref. [35]; ^{g)}Ref. [36]; ^{h)}Ref. [37]; ⁱ⁾Ref. [38]; ^{j)}Ref. [39]

3. Results and discussion

To investigate the effect of Gd doping on the work function and magnetism of $\text{Fe}_{1-x}\text{Gd}_x/\text{Fe}$ (001), different compositions of the surface layer for the $\text{Fe}_{1-x}\text{Gd}_x/\text{Fe}$ (001) system were constructed by varying the ratio of the four Gd and Fe atoms. Four doping contents with $x = 0.25, 0.50, 0.75, 1.00$ were considered. The calculated results indicated that, the Gd doping hardly influences the x and y positions of Gd and Fe atoms. In the x – y plane, the lattice constants for $x = 0.00, 0.25, 0.50, 0.75, 1.00$ stay as (2.830 ± 0.001) Å. However, the Gd doping has a great effect on their z positions. Figures 1(a)–1(e) show the side views of the atom arrangements for $\text{Fe}_{1-x}\text{Gd}_x/\text{Fe}$ (001) films with $x = 0.00, 0.25, 0.50, 0.75,$

1.00, respectively. For $x = 0.25$, the Gd atom is higher than the other three Fe atoms on the surface layer. For $x = 0.50$, both catercorner Gd atoms move outward away from the surface, and the remaining two Fe atoms are lower than the Gd atoms. For $x = 0.75$, both catercorner Gd atoms move outward away from the surface, and both the remaining Fe and Gd atoms stay lower. For $x = 1.00$, four Gd atoms all move outward away from the surface, while both catercorner Gd atoms are higher than the remaining ones. Especially, for $x \leq 0.75$, the coupling between Gd and Fe atoms is ferromagnetic. However, for $x = 1.00$, there exists antiferromagnetic coupling between Gd and Fe atoms, which is similar to the antiferromagnetic coupling between Mn and Fe for the Mn/Fe (001) film.^[30] These

results should be due to the changes of the atom arrangements aroused by the Gd doping. Figure 2 shows the exchange coupling constant (J) between Gd and Fe atoms as a function of the Gd-Fe distance. Here, $J = E_{AFM} - E_{FM}$, where E_{AFM} and E_{FM} are the total energies of the AFM and the FM states, respectively. A positive J means ferromagnetic coupling, while a negative J indicates antiferromagnetic coupling. From the figure, it is observed that the magnetic coupling between Fe and Gd atoms is sensitive to the inter-atomic distance. Especially, when $d < 3.80 \text{ \AA}$, J is positive; when $d > 3.80 \text{ \AA}$, it becomes negative. Therefore, there exists a critical Gd-Fe distance for the transition from ferromagnetic coupling to anti-

ferromagnetic coupling. As seen in Fig. 1, the distances of the nearest neighbor Gd and Fe atoms for $x \leq 0.75$ are all less than 3.80 \AA . Thus, the magnetic coupling between Gd and Fe atoms is FM with $x \leq 0.75$. However, for $x = 1.0$, there exist two high-position Gd atoms (spin down) and two low-position Gd atoms (spin up). For the high-position Gd atoms, the distance (4.587 \AA) between Gd and Fe atoms is larger than 3.80 \AA , which responds to the antiferromagnetic coupling. For the low-position Gd atoms, the distance (2.749 \AA) between Gd and Fe atoms is less than 3.80 \AA , which responds to the ferromagnetic coupling.

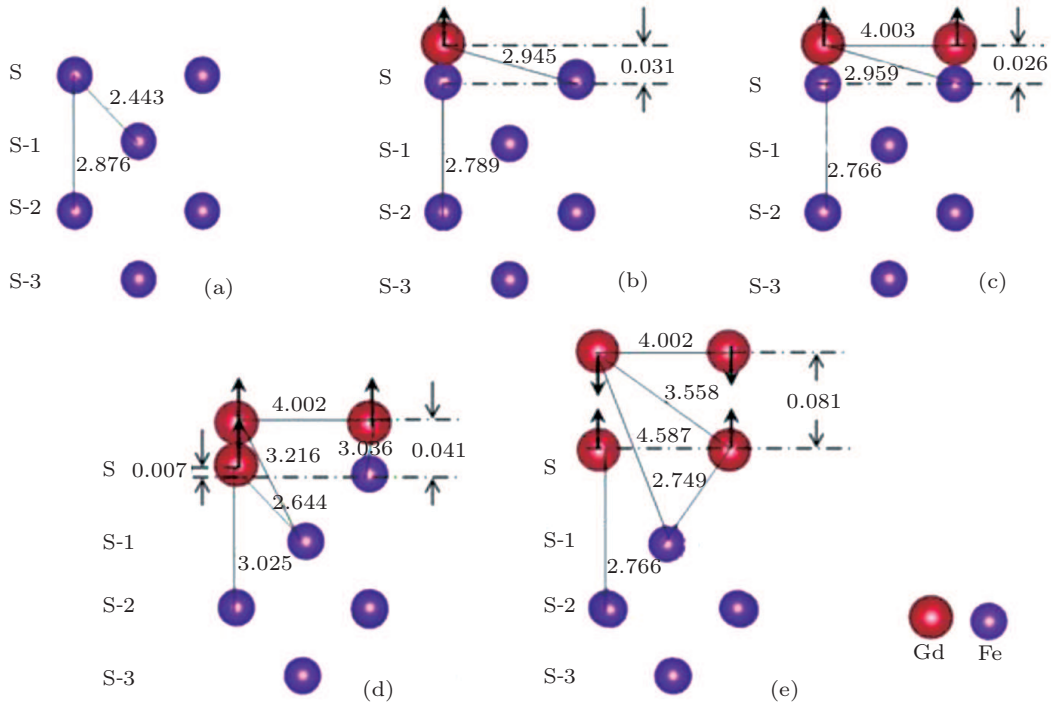


Fig. 1. (color online) Side views of the atom arrangements for the top four layers of $Fe_{1-x}Gd_x/Fe$ (001): (a) $x = 0.0$, (b) $x = 0.25$, (c) $x = 0.5$, (d) $x = 0.75$, (e) $x = 1.0$.

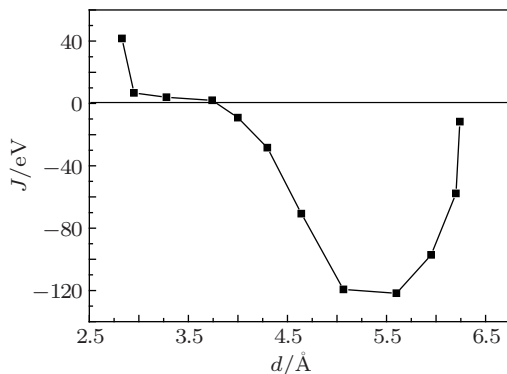


Fig. 2. Exchange coupling constant J between Gd and Fe atoms as a function of the Gd-Fe distance.

Figure 3 shows the Fermi energy and the work function as a function of Gd doping content x on the surface layer for Fe(001). From the figure, it can be found that for $x \leq 0.5$, with

increasing x , the Fermi energy is increased and the work function is decreased except for $x = 0.5$. Table 2 lists the calculated

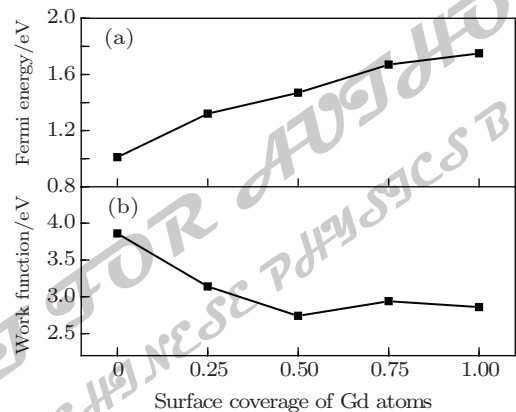


Fig. 3. (a) Fermi energy E_F and (b) work function Φ as a function of Gd doping content x on the surface layer for Fe (001).

Fermi energies E_F , work functions Φ , and magnetic moments M of the topmost three layer atoms for $\text{Gd}_x\text{Fe}_{1-x}/\text{Fe}(001)$ surfaces. As shown in Table 2, the work functions of Fe (001) can be reduced by Gd doping, which is consistent with the experimental results in Ref. [6]. It is believed that the effect of a layer of adsorbate on the work function of a surface is governed by the electronegativity of the adsorbate.^[40-43] The electronegativity of Gd (1.21) is less than that of Fe (1.83),

which results in an excess of positive charge on the surface layer and negative charge below the surface layer. This leads to a positive dipole, which gives rise to the reduction of the work function. Moreover, with the increase of the Gd doping content, the Fermi energy E_F is elevated due to the electron transfer from Gd to Fe. At the same time, the change of the Fermi energy E_F will also give rise to one of the magnetic moments of Gd and Fe atoms.

Table 2. The calculated Fermi energies E_F , work functions Φ , and magnetic moments M of the topmost three layer atoms for each $\text{Gd}_x\text{Fe}_{1-x}/\text{Fe}(001)$ film.

	x	0.0	0.25	0.5	0.75	1.0
S	$M(\text{Gd})/\mu_B$		5.015	6.74, 6.17 ($\bar{M} = 6.46$)	2.31, 7.31, 7.31 ($\bar{M} = 5.64$)	-7.65, -7.65, 6.96, 6.96 ($\bar{M} = 7.30$)
	$M(\text{Fe})/\mu_B$	2.98	2.56, 2.56, 2.97 ($\bar{M} = 2.70$)	2.10, 2.10	1.90	
S-1	$M(\text{Fe})/\mu_B$	2.27	2.24	2.21	2.22	2.38
S-2	$M(\text{Fe})/\mu_B$	2.37	2.36	2.27	2.30	2.35
	E_F/eV	1.01	1.32	1.47	1.67	1.75
	Φ/eV	3.86	3.14	2.74	2.94	2.86

Figure 4 shows the schematic density of states $N(E)$ of ferromagnetic Fe–Gd metal alloy occurring in the presence of an effective magnetic field H_{eff} ($H_{\text{eff}} = H + H_W$), where H is the external magnetic field, and H_W is the Weiss molecular field that is proportional to the exchange coupling constants. There is an energy shift of $-\mu_B H_{\text{eff}}$ ($+\mu_B H_{\text{eff}}$) for electrons with magnetic moments parallel (antiparallel) to the applied magnetic field. The electrons which flip their magnetic moments from $+\mu_B$ to $-\mu_B$ are those contained in the energy interval around the Fermi level, their number is denoted by ΔN . Then, we have^[22]

$$\Delta N = [N_{\downarrow}(E_F) + N_{\uparrow}(E_F)]\mu_B H_{\text{eff}} \times \{1 - [N_{\downarrow}(E_F) - N_{\uparrow}(E_F)]/[N_{\downarrow}(E_F) + N_{\uparrow}(E_F)]\}, \quad (1)$$

and the change of the Fermi level is given by

$$\Delta E_F = [N_{\downarrow}(E_F) - N_{\uparrow}(E_F)]\mu_B H_{\text{eff}}/[N_{\downarrow}(E_F) + N_{\uparrow}(E_F)], \quad (2)$$

where $N_{\downarrow}(E_F)$ and $N_{\uparrow}(E_F)$ are the density-of-states at the Fermi level for down and up spins, respectively. Moreover, when the electrons transfer from the surface magnetic atoms to the substrate atoms, the numbers of electrons with up and down spins filling in near the Fermi level are different. It is found that the added electrons in Fig. 4 with up spins are more than those with down spins. Therefore, with increasing the number of the transfer electrons, the net magnetic moment should be increased and the Fermi level should be ascended. As Fe is replaced by Gd, the electrons of Gd will transfer into the Fermi surface of Fe. As a result, the doping of Gd will give rise to the lifting of the Fermi energy level, the decrease of the magnetic moment of Gd, and the increase of the Fe moment.

However, compared to the results in Table 2, the Fe moments are instead reduced by the Gd doping, which means that there exist other factors influencing the Fe magnetic moment except for the electron transfer. The complex influence roles on the magnetic moment will be discussed in the following text.

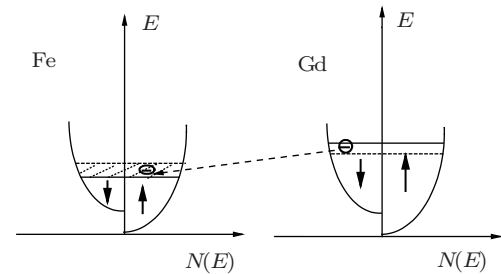


Fig. 4. Schematic density of states $N(E)$ of ferromagnetic Gd and Fe metals.

The electron transfer is an important factor affecting the work function. Figure 5 shows the contour plot of the difference of the electron density for $\text{Fe}_{1-x}\text{Gd}_x/\text{Fe}$ (001) with $x = 0.25, 0.5, 0.75$. From the figure, it can be clearly seen that there exist strong Gd–Fe and Gd–Gd interactions for each $\text{Fe}_{1-x}\text{Gd}_x/\text{Fe}$ (001) film. At the same time, for $\text{Fe}_{1-x}\text{Gd}_x/\text{Fe}$ (001) ($x = 0.25, 0.50, 0.75, 1.00$), the charge transfer from Gd to Fe leads to a positive dipole formed on the surface, which is responsible for the decrease of the work function. The change of the work function is mainly determined by the change of the Fermi level. However, the change of the surface structure can also influence the change of the work function. As shown in Fig. 1, the distance $d_{\text{Fe-Gd}}$ between the Fe layer and the Gd layer increases from 0.031 Å to 0.081 Å with the increase of

Gd doping content x , except for $x = 0.5$ with 0.026 \AA . The Gd–Fe interactions for $x = 0.5$ with least $d_{\text{Fe–Gd}}$ (0.026 \AA) are stronger than those for $x = 0.25$ and 0.75 , which leads to the highest surface positive dipole. It was reported that the change of work function $\Delta\Phi$ is proportional to the surface dipole.^[37] Therefore, the unusual reduction of the work function of $\text{Fe}_{0.5}\text{Gd}_{0.5}/\text{Fe}$ (001) should be attributed to less $d_{\text{Fe–Gd}}$.

From Table 2, it is found that the magnetic moments of Fe and Gd on the surface layer can be strongly influenced by Gd doping. As seen in Table 1, for pure Fe and Gd atoms, their surface magnetic moments are $2.98\mu_{\text{B}}$ and $7.73\mu_{\text{B}}$, respectively. On the Fe(001) surface, as one Fe atom is replaced by one Gd atom, on the one hand, the electrons of the Gd atom will be transferred into the Fermi surface of Fe, which will give rise to the decrease of the Gd magnetic moment and the increase of the Fe moment; on the other hand, the coupling interaction between Gd and Fe atoms has the Weiss molecular field H_{W} acting on the Fe atom reduced, which leads to the decrease of the Fe magnetic moment. Therefore, the combined actions of both factors above make the Gd and Fe magnetic moments

decrease. Moreover, with increasing the Gd doping content, the average moment of the Fe atom on the surface layer is further reduced. For a low Gd doping content ($x \leq 0.25$), the moment of Fe on the surface layer is higher than that for bulk Fe, which is attributed to the surface effect.^[43–46] While for $x > 0.25$, the strong Gd–Fe interaction leads to the decrease of the moment of Fe, which is consistent with the results in Ref. [47]. However, the changes of Gd magnetic moments are more complex. For all $\text{Gd}_x\text{Fe}_{1-x}/\text{Fe}$ (001) films, the average moments of Gd are lower than its surface magnetic moments ($7.73\mu_{\text{B}}$), which is due to the coupling interaction between Gd and Fe. When $x \geq 0.5$, there exist the pairing Gd atoms moving outward away from the surface, as seen in Fig. 1. The magnetic moments of the pairing Gd atoms above are near the surface magnetic moments of Gd, which is attributed to a strong Gd–Gd interaction and a weak Gd–Fe interaction. For $x = 0.75$, there are two pairing Gd atoms at higher levels and one Gd atom at lower levels. Moreover, the Gd atom at lower levels has a small magnetic moment with $M = 2.31\mu_{\text{B}}$ due to the strong Gd–Fe coupling.

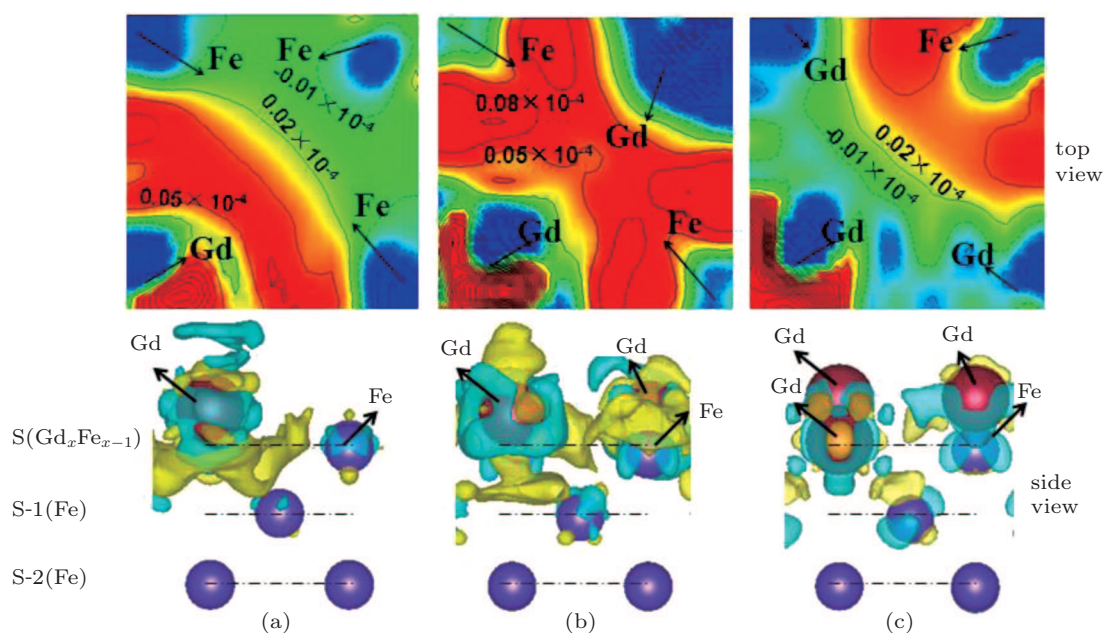


Fig. 5. (color online) Contour plot of the difference of the electron density (in $e/\text{\AA}^3$) for (a) $x = 0.25$, (b) $x = 0.5$, and (c) $x = 0.75$. Solid and dashed lines are used to label contours whose values are larger and less than zero for the 2D maps of the top view, while in 3D maps of the side view for the top three layers, positive and negative values are shown by yellow and blue, respectively.

4. Conclusion

In conclusion, we have investigated the effects of the Gd doping on the magnetism and work function of $\text{Fe}_{1-x}\text{Gd}_x/\text{Fe}$ (001). It is found that the Gd doping gives rise to the restructuring of the surface atoms of $\text{Fe}_{1-x}\text{Gd}_x/\text{Fe}$ (001), which leads to the transition of magnetic coupling between Gd and Fe atoms from FM with $x \leq 0.75$ to mixed AFM and FM with $x = 1.00$. As the Fe atoms are replaced by the Gd atoms, the charge

transfer from Gd to Fe appears. The electronegativity of Gd is less than that of Fe, which leads to a positive dipole. This is responsible for the decrease of the work function with increasing Gd doping content. Moreover, it is found that the electron transfer, Gd–Gd and Gd–Fe couplings do jointly determine the changes of the magnetic moments of Fe and Gd on the surface layer. Of course, after Gd doping, the complex surface restructuring should be one of the main origins of the various changes of Gd and Fe magnetic moments.

References

- [1] Schmidt G, Ferrand D, Molenkamp L W, Filip A T and Van Wees B J 2000 *Phys. Rev. B* **62** R4790
- [2] Rashba E I 2000 *Phys. Rev. B* **62** R16267
- [3] Fert A and Jaffrès H 2001 *Phys. Rev. B* **64** 184420
- [4] Dash S P, Sharma S, Patel R S, de Jong M P and Jansen R 2009 *Nature* **462** 491
- [5] Min B C, Motohashi K, Lodder C and Jansen R 2006 *Nat. Mater.* **5** 817
- [6] Zenkevich A V, Matveyev Y A, Lebedinskii Y Y, Mantovan R, Fanciulli, Thiess M S and Drube W 2012 *J. Appl. Phys.* **111** 07C506
- [7] Wang B M, Ru G P, Jiang Y L, Qu X P, Li B Z and Liu R 2008 *Micro-electronic Engineering* **85** 2032
- [8] Ishii R, Matsumura K, Sakai A and Sakata T 2001 *Appl. Surf. Sci.* **169**–**170** 658
- [9] Tsui B Y 2003 *IEEE Electron. Device Lett.* **24** 153
- [10] Xu G G, Wu Q Y, Chen Z G, Huang Z G, Wu R Q and Feng Y P 2008 *Phys. Rev. B* **78** 115420
- [11] Xu G G, Wu Q Y, Chen Z G, Huang Z G and Feng Y P 2009 *J. Appl. Phys.* **106** 043708
- [12] Park S, Colombo L, Nishi Y and Cho K 2005 *Appl. Phys. Lett.* **86** 073118
- [13] Payne M C, Teter M P, Allan D C, Arias T A and Joannopoulos J D 1992 *Rev. Mod. Phys.* **64** 1045
- [14] Kresse G and Furthmüller J 1996 *Comput. Mater. Sci.* **6** 15
- [15] Kresse G and Joubert D 1999 *Phys. Rev. B* **59** 1758
- [16] Blöchl P E 1994 *Phys. Rev. B* **50** 17953
- [17] Perdew J P, Burke K and Ernzerhof M 1996 *Phys. Rev. Lett.* **77** 3865
- [18] Xu G G, Wu J, Chen Z G, Lin Y B and Huang Z G 2012 *Chin. Phys. B* **21** 097401
- [19] Xu G G, Wu Q Y, Zhang J M, Chen Z G and Huang Z G 2009 *Acta Phys. Sin.* **58** 1924 (in Chinese)
- [20] Zhong K H, Weng Z Z, Feng Q, Yang Y M and Huang Z G 2011 *Chin. Phys. Lett.* **28** 057501
- [21] Lu P X and Qu L B 2013 *Chin. Phys. Lett.* **30** 17101
- [22] Zhong K H, Xu G G, Cheng Y M, Tang K Q, Chen Z G and Huang Z G 2012 *AIP Adv.* **2** 042134
- [23] Anisimov V I, Solovyev I V, Korotin M A, Czyzyk M T and Sawatzky G A 1993 *Phys. Rev. B* **48** 16929
- [24] Anisimov V I, Korotin M A, Zaanen J and Andersen O K 1991 *Phys. Rev. B* **44** 943
- [25] Dudarev S L, Botton G A, Savrasov S Y, Humphreys C J and Sutton A P 1998 *Phys. Rev. B* **57** 1505
- [26] Bantounas I, Goumri-Said S, Kanoun M B, Manchon A, Roqan I and Schwingschlögl U 2011 *J. Appl. Phys.* **109** 083929
- [27] Methfessel M and Paxton A T 1989 *Phys. Rev. B* **40** 3616
- [28] Press W H, Flannery B P, Teukolsky S A and Vetterling W T 1986 *New Numerical Recipes* (2nd edn.) (Cambridge: Cambridge University Press)
- [29] Lang N D and Kohn W 1971 *Phys. Rev. B* **3** 1215
- [30] Hafner J and Spišák D 2005 *Phys. Rev. B* **72** 144420
- [31] Acet M, Zahres H, Wassermann E F and Pepperhoff W 1994 *Phys. Rev. B* **49** 6012
- [32] Kittel C 1996 *Introduction to Solid State Physics* (7th edn.) (New York: John Wiley & Sons, Inc.)
- [33] Turner A M, Chang Y J and Erskine J L 1982 *Phys. Rev. Lett.* **48** 348
- [34] Blonski P and Kiejna A 2004 *Vacuum* **74** 179
- [35] Paggel J J, Wei C M, Chou M Y, Luh D A, Miller T and Chiang T C 2002 *Phys. Rev. B* **66** 233403
- [36] Beaudry B J and Gschneider K A 1982 *Handbook on the Physics and Chemistry of Rare Earth's* **1** 216
- [37] Roeland L W, Cock G J, Muller F A, Moleman A C, McEwen K A, Jordanl R G and Jone D W 1975 *J. Phys. F: Metal Phys.* **5** L233
- [38] Shick A B, Pickett W E and Fadley C S 2000 *Phys. Rev. B* **61** R9213
- [39] Michaelson H B 1977 *J. Appl. Phys.* **48** 4729
- [40] Leung T C, Kao C L, Su W S, Feng Y J and Chan C T 2003 *Phys. Rev. B* **68** 195408
- [41] Huang S F, Chang R S, Leung T C and Chan C T 2005 *Phys. Rev. B* **72** 075433
- [42] Black-Schaffer A M and Cho K 2006 *J. Appl. Phys.* **100** 124902
- [43] Huang Z G and Du Y W 2002 *Phys. Lett. A* **300** 641
- [44] Ramanathan A A, Khalifeh J M and Hamad B A 2008 *J. Magn. Magn. Mater.* **320** 2629
- [45] Freeman A J and Wu R Q 1991 *J. Magn. Magn. Mater.* **100** 497
- [46] Wang C S and Freeman A J 1981 *Phys. Rev. B* **24** 4364
- [47] Sajjeddine M, Bauer P, Cherifi K, Dufour C and Marchal G 1994 *Phys. Rev. B* **49** 8815

JUST FOR AUTHORS
— CHINESE PHYSICS B

Chinese Physics B

Volume 23

Number 5

May 2014

TOPICAL REVIEW — Magnetism, magnetic materials, and interdisciplinary research

057505 Nanomagnetism: Principles, nanostructures, and biomedical applications

Yang Ce, Hou Yang-Long and Gao Song

058106 Progress in organic spintronics

Yang Fu-Jiang, Han Shi-Xuan and Xie Shi-Jie

RAPID COMMUNICATION

054301 Manipulation of extraordinary acoustic transmission by a tunable bull's eye structure

Wang Ji-Wei, Cheng Ying and Liu Xiao-Jun

GENERAL

050201 Collective surrounding control in multi-agent networks

Wei Ting-Ting and Chen Xiao-Ping

050202 A high order energy preserving scheme for the strongly coupled nonlinear Schrödinger system

Jiang Chao-Long and Sun Jian-Qiang

050203 A new coupled map car-following model considering drivers' steady desired speed

Zhou Tong, Sun Di-Hua, Li Hua-Min and Liu Wei-Ning

050301 Statistical properties of coherent photon-subtracted two-mode squeezed vacuum and its application in quantum teleportation

Zhang Guo-Ping, Zheng Kai-Min, Liu Shi-You and Hu Li-Yun

050302 Ocean internal waves interpreted as oscillation travelling waves in consideration of ocean dissipation

Jiang Zhu-Hui, Huang Si-Xun, You Xiao-Bao and Xiao Yi-Guo

050303 Doppler shift of a laser pulse beam scattered by a rotating cone and cylinder

Wang Bao-Ping, Wang Ming-Jun, Wu Zhen-Sen, Li Ying-Le and Xiang Ning-Jing

050304 Thermal quantum and total correlations in spin-1 bipartite system

Qiu Liang and Ye Bin

050305 Thermal entanglement in the mixed three-spin XXZ Heisenberg model on a triangular cell

Seyit Deniz Han and Ekrem Aydinler

050306 Complete hyperentangled state analysis and generation of multi-particle entanglement based on charge detection

Ji Yan-Qiang, Jin Zhao, Zhu Ai-Dong, Wang Hong-Fu and Zhang Shou

050307 Cavity-assisted quantum computing in a silicon nanostructure

Tang Bao, Qin Hao, Zhang Rong, Liu Jing-Ming and Xue Peng

(Continued on the Bookbinding Inside Back Cover)

- 050308** Consequent entanglement concentration of a less-entangled electronic cluster state with controlled-not gates
Zhou Lan
- 050309** Measures of genuine multipartite entanglement for graph states
Guo Qun-Qun, Chen Xiao-Yu and Wang Yun-Yun
- 050310** Measurement-induced disturbance in Heisenberg XY spin model with Dzialoshinskii–Moriya interaction under intrinsic decoherence
Shen Cheng-Hao, Zhang Guo-Feng, Fan Kai-Ming and Zhu Han-Jie
- 050311** Spin-star environment assisted entanglement generation in weakly coupled bipartite systems
Wang Gen-Fang, Lü Jian-Mei and Wang Lin-Cheng
- 050401** Mechanical properties of the thermal equilibrium Friedmann–Robertson–Walker universe model
Wei Yi-Huan, Lan Tian-Bao, Zhang Yue-Zhu and Fu Yan-Yan
- 050501** A statistical model for predicting thermal chemical reaction rate
Lin Zheng-Zhe, Li Wang-Yao and Ning Xi-Jing
- 050502** Motion of spiral tip driven by local forcing in excitable media
Liu Gui-Quan and Ying He-Ping
- 050503** Adaptive step-size modified fractional least mean square algorithm for chaotic time series prediction
Bilal Shoaib, Ijaz Mansoor Qureshi, Shafqatullah and Ihsanulhaq
- 050504** A new approach of optimal control for a class of continuous-time chaotic systems by an online ADP algorithm
Song Rui-Zhuo, Xiao Wen-Dong and Wei Qing-Lai
- 050505** Generation of a novel spherical chaotic attractor from a new three-dimensional system
Sun Chang-Chun, Zhao En-Liang and Xu Qi-Cheng
- 050506** Collective dynamics in a non-dissipative two-coupled pendulum system
Chen Zi-Chen, Li Bo, Qiu Hai-Bo and Xi Xiao-Qiang
- 050507** Hyper-chaos encryption using convolutional masking and model free unmasking
Qi Guo-Yuan and Sandra Bazebo Matondo
- 050508** Linear and nonlinear generalized consensus of multi-agent systems
Guo Liu-Xiao, Hu Man-Feng, Hu Ai-Hua and Xu Zhen-Yuan
- 050509** Pinning sampled-data synchronization for complex networks with probabilistic coupling delay
Wang Jian-An, Nie Rui-Xing and Sun Zhi-Yi
- 050510** Synchronization transition of a coupled system composed of neurons with coexisting behaviors near a Hopf bifurcation
Jia Bing
- 050511** Complex solutions and novel complex wave localized excitations for the (2+1)-dimensional Boiti–Leon–Pempinelli system
Ma Song-Hua, Xü Gen-Hai and Zhu Hai-Ping
- 050512** Exit selection strategy in pedestrian evacuation simulation with multi-exits
Yue Hao, Zhang Bin-Ya, Shao Chun-Fu and Xing Yan

(Continued on the Bookbinding Inside Back Cover)

050513 Output power analyses for the thermodynamic cycles of thermal power plants

Sun Chen, Cheng Xue-Tao and Liang Xin-Gang

050701 Cellular automata model for traffic flow with safe driving conditions

María Elena Lárraga and Luis Alvarez-Icaza

ATOMIC AND MOLECULAR PHYSICS

053101 Spectroscopic properties and radiative lifetimes of SiTe: A high-level multireference configuration interaction investigation

Li Rui, Zhang Xiao-Mei, Jin Ming-Xing, Xu Hai-Feng and Yan Bing

053201 Probing dynamic interference in high-order harmonic generation from long-range molecular ion: Bohmian trajectory investigation

Wang Jun, Wang Bing-Bing, Guo Fu-Ming, Li Su-Yu, Ding Da-Jun, Chen Ji-Gen, Zeng Si-Liang and Yang Yu-Jun

053202 Investigation on the influence of atomic potentials on the above threshold ionization

Tian Yuan-Ye, Li Su-Yu, Wei Shan-Shan, Guo Fu-Ming, Zeng Si-Liang, Chen Ji-Gen and Yang Yu-Jun

053401 Projectile electron loss in collisions of light charged ions with helium

Yin Yong-Zhi, Wang Yun and Chen Xi-Meng

053402 Electron impact ionization of neon and neon ions under distorted-wave Born approximation

Zhou Li-Xia and Yan You-Guo

053403 Decay pathways of superexcited states of nitrous oxide

Lin Mei, Liu Ya-Wei, Zhong Zhi-Ping and Zhu Lin-Fan

ELECTROMAGNETISM, OPTICS, ACOUSTICS, HEAT TRANSFER, CLASSICAL MECHANICS, AND FLUID DYNAMICS

054101 Design of two-dimensional elliptically cylindrical invisible cloaks with multiple regions

Luo Xiao-Yang, Liu Dao-Ya, Liu Jin-Jing and Dong Jian-Feng

054102 Inverse design-based metamaterial transparent device and its multilayer realization

Li Ting-Hua, Huang Ming, Yang Jing-Jing, Yuan Gang and Cai Guang-Hui

054103 The polarization effect of a laser in multiphoton Compton scattering

Liang Guo-Hua, Lü Qing-Zheng, Teng Ai-Ping and Li Ying-Jun

054201 Scattering and propagation of terahertz pulses in random soot aggregate systems

Li Hai-Ying, Wu Zhen-Sen, Bai Lu and Li Zheng-Jun

054202 Subwavelength Fourier-transform imaging without a lens or a beamsplitter

Liu Rui-Feng, Yuan Xin-Xing, Fang Yi-Zhen, Zhang Pei, Zhou Yu, Gao Hong and Li Fu-Li

054203 Correspondence normalized ghost imaging on compressive sensing

Zhao Sheng-Mei and Zhuang Peng

054204 Transient responses of transparency in a far-off resonant atomic system

Hu Zheng-Feng, Du Chun-Guang, Deng Jian-Liao and Wang Yu-Zhu

- 054205 Off-resonant double-resonance optical-pumping spectra and their application in a multiphoton cesium magneto-optical trap**
Yang Bao-Dong, He Jun and Wang Jun-Min
- 054206 Switching from positive to negative absorption with electromagnetically induced transparency in circuit quantum electrodynamics**
Li Hai-Chao and Ge Guo-Qin
- 054207 Diode-pumped self-starting mode-locked femtosecond Yb:YCa₄O(BO₃)₃ laser**
Gao Zi-ye, Zhu Jiang-Feng, Tian Wen-Long, Wang Jun-Li, Wang Qing, Zhang Zhi-Guo, Wei Zhi-Yi, Yu Hao-Hai, Zhang Huai-Jin and Wang Ji-Yang
- 054208 A novel 2- μ m pulsed fiber laser based on a supercontinuum source and its application to mid-infrared supercontinuum generation**
Yang Wei-Qiang, Zhang Bin, Hou Jing, Yin Ke and Liu Ze-Jin
- 054209 Multi-component optical azimuthons of four-wave mixing**
Wang Rui-Min, Wang Xing-Peng, Wu Zhen-Kun, Yao Xin, Zhang Yi-Qi and Zhang Yan-Peng
- 054210 Low-loss terahertz waveguide with InAs-graphene-SiC structure**
Xu De-Gang, Wang Yu-ye, Yu Hong, Li Jia-Qi, Li Zhong-Xiao, Yan Chao, Zhang Hao, Liu Peng-Xiang, Zhong Kai, Wang Wei-Peng and Yao Jian-Quan
- 054211 Influence of barrier thickness on the structural and optical properties of InGaN/GaN multiple quantum wells**
Liang Ming-Ming, Weng Guo-En, Zhang Jiang-Yong, Cai Xiao-Mei, Lü Xue-Qin, Ying Lei-Ying and Zhang Bao-Ping
- 054302 Molecular structure dependence of acoustic nonlinearity parameter B/A for silicone oils**
Zhang Zhe, Chen Gong and Zhang Dong
- 054501 Noether symmetry and conserved quantity for a Hamilton system with time delay**
Jin Shi-Xin and Zhang Yi
- 054502 Reactionless robust finite-time control for manipulation of passive objects by free-floating space robots**
Guo Sheng-Peng, Li Dong-Xu, Meng Yun-He and Fan Cai-Zhi
- 054503 Properties of surface waves in granular media under gravity**
Zheng He-Peng
- 054701 MHD flow of nanofluids over an exponentially stretching sheet in a porous medium with convective boundary conditions**
T. Hayat, M. Imtiaz, A. Alsaedi and R. Mansoor
- 054702 Existence of a Hartmann layer in the peristalsis of Sisko fluid**
Saleem Asghar, Tayyaba Minhas and Aamir Ali
- 054703 Newtonian heating effects in three-dimensional flow of viscoelastic fluid**
A. Qayyum, T. Hayat, M. S. Alhuthali and H. M. Malaikah

(Continued on the Bookbinding Inside Back Cover)

PHYSICS OF GASES, PLASMAS, AND ELECTRIC DISCHARGES

- 055101** Validity of the two-term Boltzmann approximation employed in the fluid model for high-power microwave breakdown in gas

Zhao Peng-Cheng, Liao Cheng, Yang Dan and Zhong Xuan-Ming

- 055201** Numerical simulation of electron cyclotron current drive characteristics on EAST

Wei Wei, Ding Bo-Jiang, Zhang Xin-Jun, Wang Xiao-Jie, Li Miao-Hui, Kong Er-Hua and Zhang Lei

- 055202** Effect of inner-surface roughness of conical target on laser absorption and fast electron generation

Wang Huan, Cao Li-Hua, Zhao Zong-Qing, Yu Ming-Yang, Gu Yu-Qiu and He Xian-Tu

CONDENSED MATTER: STRUCTURAL, MECHANICAL, AND THERMAL PROPERTIES

- 056101** Icosahedral quasicrystals solids with an elliptic hole under uniform heat flow

Li Lian-He and Liu Guan-Ting

- 056102** Finite size specimens with cracks of icosahedral Al–Pd–Mn quasicrystals

Yang Lian-Zhi, Ricoeur Andreas, He Fan-Min and Gao Yang

- 056103** Coulombic interaction in the colloidal oriented-attachment growth of tetragonal nanorods

Li Jun-Fan, Wen Ke-Chun, He Wei-Dong, Wang Xiao-Ning, Lü Wei-Qiang, Yan Peng-Fei, Song Yuan-Qiang, Lu Hong-Liang, Lin Xiao and Dickerson J. H.

- 056104** Role of helium in the sliding and mechanical properties of a vanadium grain boundary: A first-principles study

Zhou Hong-Bo, Jin Shuo, Zhang Ying, Shu Xiao-Lin and Niu Liang-Liang

- 056201** Controllable synthesis of high aspect ratio $\text{Mg}_2\text{B}_2\text{O}_5$ nanowires and their applications in reinforced polyhydroxyalkanoate composites

Mo Zhao-Jun, Chen Jin-Peng, Lin Jing, Fan Ying, Liang Chun-Yong, Wang Hong-Shui, Xu Xue-Wen, Hu Long and Tang Cheng-Chun

- 056301** Effect of Gd doping on the magnetism and work function of $\text{Fe}_{1-x}\text{Gd}_x/\text{Fe}$ (001)

Tang Ke-Qin, Zhong Ke-Hua, Cheng Yan-Min and Huang Zhi-Gao

- 056701** Diverse solid and supersolid phases of bosons in a triangular lattice

Chen Qi-Hui and Li Peng

- 056801** Corrosion related properties of iron (100) surface in liquid lead and bismuth environments: A first-principles study

Song Chi, Li Dong-Dong, Xu Yi-Chun, Pan Bi-Cai, Liu Chang-Song and Wang Zhi-Guang

CONDENSED MATTER: ELECTRONIC STRUCTURE, ELECTRICAL, MAGNETIC, AND OPTICAL PROPERTIES

- 057101** First-principles study of the influences of oxygen defects upon the electronic properties of Nb-doped TiO_2 by GGA + U methods

Song Chen-Lu, Yang Zhen-Hui, Su Ting, Wang Kang-Kai, Wang Ju, Liu Yong and Han Gao-Rong

- 057102** 4H-SiC Schottky barrier diodes with semi-insulating polycrystalline silicon field plate termination

Yuan Hao, Tang Xiao-Yan, Zhang Yi-Men, Zhang Yu-Ming, Song Qing-Wen, Yang Fei and Wu Hao

- 057103 Rectifying and photovoltaic properties of ZnCo₂O₄/Si heterostructure grown by pulsed laser deposition**
Chen Zhao, Wen Xiao-Li, Niu Li-Wei, Duan Meng-Meng, Zhang Yun-Jie, Dong Xiang-Lei and Chen Chang-Le
- 057104 Electronic and optical properties of Au-doped Cu₂O: A first principles investigation**
Jiang Zhong-Qian, Yao Gang, An Xin-You, Fu Ya-Jun, Cao Lin-Hong, Wu Wei-Dong and Wang Xue-Min
- 057201 Detection of Majorana fermions in an Aharonov–Bohm interferometer**
Shang En-Ming, Pan Yi-Ming, Shao Lu-Bing and Wang Bai-Geng
- 057202 Effect of charge order transition on tunneling resistance in Pr_{0.6}Ca_{0.4}MnO₃/Nb-doped SrTiO₃ hetero-junction**
Wang Deng-Jing, Ma Jun-Jie, Wang Mei, Wang Ru-Wu and Li Yun-Bao
- 057203 Experimental and numerical analyses of high voltage 4H-SiC junction barrier Schottky rectifiers with linearly graded field limiting ring**
Wang Xiang-Dong, Deng Xiao-Chuan, Wang Yong-Wei, Wang Yong, Wen Yi and Zhang Bo
- 057204 High performance oscillator with 2-mW output power at 300 GHz**
Wu De-Qi, Ding Wu-Chang, Yang Shan-Shan, Jia Rui, Jin Zhi and Liu Xin-Yu
- 057205 Fabrication and electrochemical performance of graphene–ZnO nanocomposites**
Li Zhen-Peng, Men Chuan-Ling, Wang Wan and Cao Jun
- 057301 Interface states in Al₂O₃/AlGaIn/GaN metal-oxide-semiconductor structure by frequency dependent conductance technique**
Liao Xue-Yang, Zhang Kai, Zeng Chang, Zheng Xue-Feng, En Yun-Fei, Lai Ping and Hao Yue
- 057302 Phonon-dependent transport through a serially coupled double quantum dot system**
M. Bagheri Tagani and H. Rahimpour Soleimani
- 057303 Effect of additional silicon on titanium/4H-SiC contacts properties**
Zhang Yong-Ping, Chen Zhi-Zhan, Lu Wu-Yue, Tan Jia-Hui, Cheng Yue and Shi Wang-Zhou
- 057304 Flat-roof phenomenon of dynamic equilibrium phase in the negative bias temperature instability effect on a power MOSFET**
Zhang Yue, Zhuo Qing-Qing, Liu Hong-Xia, Ma Xiao-Hua and Hao Yue
- 057305 Model of hot-carrier induced degradation in ultra-deep sub-micrometer nMOSFET**
Lei Xiao-Yi, Liu Hong-Xia, Zhang Yue, Ma Xiao-Hua and Hao Yue
- 057401 Parallel variable-density spiral imaging using nonlocal total variation reconstruction**
Fang Sheng and Guo Hua
- 057402 Josephson current versus potential strength of the interface in ferromagnetic superconductors**
Hamidreza Emamipour
- 057403 Magnetic property improvement of niobium doped with rare earth elements**
Jiang Tao, He Fei-Si, Jiao Fei, He Fa, Lu Xiang-Yang, Zhao Kui, Zhao Hong-Yun, You Yu-Song and Chen Lin
- 057501 Monte Carlo study of the magnetic properties of spin liquid compound NiGa₂S₄**
Zhang Kai-Cheng, Li Yong-Feng, Liu Yong and Chi Feng
- 057502 Dielectric behavior of Cu–Zn ferrites with Si additive**
Uzma G

- 057503 High sum-frequency generation in dielectric/antiferromagnet/Ag sandwich structures**
Fu Shu-Fang, Liang Hong, Zhou Sheng and Wang Xuan-Zhang
- 057504 A new aluminum iron oxide Schottky photodiode designed via sol-gel coating method**
A. Tataroğlu, A. A. Hendi, R. H. Alorainy and F. Yakuphanoglu
- 057801 Photoluminescence properties and energy transfer in $Y_2O_3:Eu^{3+}$ nanophosphors**
Cui Hang, Zhu Pei-Fen, Zhu Hong-Yang, Li Hong-Dong and Cui Qi-Liang
- 057802 Up-conversion luminescence properties and energy transfer of Er^{3+}/Yb^{3+} co-doped oxyfluoride glass ceramic containing CaF_2 nano-crystals**
Ma Chen-Shuo, Jiao Qing, Li Long-Ji, Zhou Da-Cheng, Yang Zheng-Wen, Song Zhi-Guo and Qiu Jian-Bei
- 057803 Effects of thermal annealing on the properties of N-implanted ZnS films**
Xue Shu-Wen, Zhang Jun and Quan Jun
- 057804 Effects of oblique incidence on terahertz responses of planar split-ring resonators**
Pan Xue-Cong, Xia Xiao-Xiang and Wang Li
- INTERDISCIPLINARY PHYSICS AND RELATED AREAS OF SCIENCE AND TECHNOLOGY**
- 058101 GaN hexagonal pyramids formed by a photo-assisted chemical etching method**
Zhang Shi-Ying, Xiu Xiang-Qian, Hua Xue-Mei, Xie Zi-Li, Liu Bin, Chen Peng, Han Ping, Lu Hai, Zhang Rong and Zheng You-Dou
- 058102 Dual-band and polarization-insensitive terahertz absorber based on fractal Koch curves**
Ma Yan-Bing, Zhang Huai-Wu, Li Yuan-Xun, Wang Yi-Cheng, Lai Wei-En and Li Jie
- 058103 Synthesis and room-temperature NO_2 gas sensing properties of a WO_3 nanowires/porous silicon hybrid structure**
Zeng Peng, Zhang Ping, Hu Ming, Ma Shuang-Yun and Yan Wen-Jun
- 058104 Structural and photoluminescence properties of terbium-doped zinc oxide nanoparticles**
Ningthoujam Surajkumar Singh, Shougaijam Dorendrajit Singh and Sanoujam Dhiren Meetei
- 058105 Structural and electrical characterization of annealed $Si_{1-x}C_x/SiC$ thin film prepared by magnetron sputtering**
Huang Shi-Hua and Liu Jian
- 058201 A voltage-controlled chaotic oscillator based on carbon nanotube field-effect transistor for low-power embedded systems**
Van Ha Nguyen, Wonkyeong Park, Namtae Kim and Hanjung Song
- 058501 Multi-polar resistance switching and memory effect in copper phthalocyanine junctions**
Qiao Shi-Zhu, Kang Shi-Shou, Qin Yu-Feng, Li Qiang, Zhong Hai, Kang Yun, Yu Shu-Yun, Han Guang-Bing, Yan Shi-Shen and Mei Liang-Mo
- 058502 Enhanced performance of GaN-based light-emitting diodes with InGaN/GaN superlattice barriers**
Cai Jin-Xin, Sun Hui-Qing, Zheng Huan, Zhang Pan-Jun and Guo Zhi-You
- 058701 High-power terahertz pulse sensor with overmoded structure**
Wang Xue-Feng, Wang Jian-Guo, Wang Guang-Qiang, Li Shuang and Xiong Zheng-Feng

058901 A conditioned level-set method with block-division strategy to flame front extraction based on OH-PLIF measurements

Han Yue, Cai Guo-Biao, Xu Xu, Renou Bruno and Boukhalifa Abdelkrim

058902 Biham–Middleton–Levine model in consideration of cooperative willingness

Pan Wei, Xue Yu, Zhao Rui and Lu Wei-Zhen

GEOPHYSICS, ASTRONOMY, AND ASTROPHYSICS

059201 Improved method for analyzing quasi-optical launchers

Wu Ze-Wei, Li Hao, Xu Jian-Hua, Li Tian-Ming and Li Jia-Yin

059202 Predicting extreme rainfall over eastern Asia by using complex networks

He Su-Hong, Feng Tai-Chen, Gong Yan-Chun, Huang Yan-Hua, Wu Cheng-Guo and Gong Zhi-Qiang

JUST FOR AUTHORS
— CHINESE PHYSICS B